NANO · MICRO small
www.small-journal.com

Check for updates

# Neoadjuvant Chemotherapy Based on Abraxane/Human Neutrophils Cytopharmaceuticals with Radiotherapy for Gastric Cancer

*Caoyun Ju, Yajing Wen, Luping Zhang, Qianqian Wang, Lingjing Xue, Jian Shen, and Can Zhang**

**Gastric cancer remains one of the most lethal cancers with high incidence and mortality worldwide. The majority of gastric cancer patients are those who have first been diagnosed in advanced stage, in which the standard chemo-radiotherapy produces limited benefit along with severe general toxicity, thus the demand for improved therapeutic efficacy and decreased side effects drives the development of novel therapeutic strategies. Here, a neoadjuvant chemotherapy based on Abraxane/human neutrophils (NEs) cytopharmaceuticals with radiotherapy is presented for effective cancer treatment. Human NEs, the most abundant white blood cells in peripheral blood, are developed to carry Abraxane, the commercial albumin-bound paclitaxel nanoparticle, to form cytopharmaceuticals (Abraxane/NEs) which have been confirmed to maintain the intrinsic functions of human NEs. The modest radiation is applied not only to exert tumor disruption, but also to increase the release of inflammatory factors which guide the NEs homing to the tumoral sites. These amplified inflammatory factors at tumor sites excessively activate Abraxane/NEs to form neutrophil extracellular traps, along with a burst release of Abraxane to induce superior tumor suppression. This adjuvant chemo-radiotherapy based on cytopharmaceuticals may provide new opportunities for advanced cancer treatment, which reveals the huge clinical potential of human neutrophils as drug delivery vectors.**

## 1. Introduction

Gastric cancer is currently the fifth most commonly diagnosed cancer worldwide and accounting for more than 720 000 deaths annually.[1] Despite an advancement in pathogenesis elucidation and therapeutic strategies have ameliorated the high incidence and mortality of patients with gastric cancer, most patients once diagnosed have been at the late-stage owing to lack of efficient early detection and primary prevention.[1b,2] The advanced gastric cancer is characterized by high tendency of tissue invasion and metastasis where surgical management usually fails, therefore the adjuvant chemo-radiotherapy treatment seems optimal for improving survival.[3] Currently, for those unresectable cancers, palliative chemotherapy regimens based on tumor progression are clinically preferred for extending patients lifetime,[2b,4] while local radiation behaves as a supplement and contribution to antitumor effect of chemotherapy.[5] Nevertheless, some crucial dilemmas of chemo-radiotherapy, such as the limited tumor-targeting of chemotherapeutics and undesired systemic side effects,[6] restrict the antitumor efficacy, thereby driving the development of novel therapeutic strategies.

It is worth noting that targeted therapies have been springing up in recent years. For example, HER2-targeted Trastuzumab has been demonstrated to have apparent survival extension, but only benefits the limited human epidermal growth factor receptor 2 (HER2)-positive gastric cancer patients.[3a,7] Nanoparticles-based drug delivery systems also perform an increased tumor-targeting of cytotoxic drugs, however, the nonspecific distribution caused by reticuloendothelial-system increases the toxicity risk to normal tissues, and the recognition of tumor relying on the receptor–ligand interaction decreases tumor-targeting efficacy.[8] Based on that, endogenous cell-based delivery platforms have been proposed as a strong potential strategy for targeting chemotherapy.[9] Neutrophils (NEs), the most abundant white blood cells in peripheral blood, possess the natural chemotaxis to inflammatory signals.[10] Amounts of NEs have been found infiltrating into the gastric tumor sites especially with *Helicobacter pylori* infection,[11] which show a positive effect on the recruitment of NEs due to the inherent pathological inflammation of gastric cancer. More importantly, chemotherapy

Dr. C. Ju, Y. Wen, L. Zhang, Q. Wang, Dr. L. Xue, Prof. C. Zhang
State Key Laboratory of Natural Medicines and Jiangsu Key Laboratory of Drug Discovery for Metabolic Diseases
Center of Advanced Pharmaceuticals and Biomaterials
China Pharmaceutical University
Nanjing 210009, P. R. China
E-mail: zhangcan@cpu.edu.cn
Prof. J. Shen
Jiangsu Collaborative Innovation Center of Biomedical Functional Materials
Nanjing Normal University
Nanjing 210046, P. R. China
The ORCID identification number(s) for the author(s) of this article can be found under https://doi.org/10.1002/smll.201804191.

DOI: 10.1002/smll.201804191


© 2018 WILEY-VCH Verlag GmbH & Co. KGaA, Weinheim

drug loaded murine NEs in response to inflammation signals have been indicated to have efficient tumor-targeting and superior biological safety in mice.[9a] However, whether human NEs can work equivalently allows for further verification. In addition, it is inspiring to find that local radiotherapy leads to the local inflammation accompany with the release of the inflammatory factor, such as interleukin-8 (IL-8),[12] which has the potential to prime NEs for migrating to the tumor sites under the radiation exposure.

Herein, we develop a neoadjuvant therapy based on human NEs cytopharmaceuticals containing Abraxane combined with radiotherapy for effective gastric cancer treatment (**Figure 1**). Abraxane, the nanoparticle albumin-bound paclitaxel (PTX), is a potential second-line chemotherapeutic for advanced gastric cancer on account of the recognized clinical efficacy such as improved antitumor effect of PTX and decreased side effects,[13] of which the albumin component works for facilitating tumor cellular uptake through the surface receptor secreted protein acidic and rich in cysteine.[14] The human NEs are isolated from the peripheral blood, followed by the internalization of Abraxane to form the cytopharmaceuticals (Abraxane/NEs) which aim to investigate the clinical potentials of human NEs as nanodrug carriers. After local radiotherapy, modest radiation can not only generate tumor destruction, but also enlarge the expression of inflammatory factors which are potential to prime NEs homing to the tumor sites.[12a] Abraxane/NEs can responsd to and migrate along the amplified inflammatory signals triggered by local radiation, followed by accumulation and excessive activation at tumor sites to form the neutrophils extracellular traps (NETs) with a concomitant release of Abraxane which can be internalized by neighboring tumor cells, and thus producing a robust antitumor efficiency.

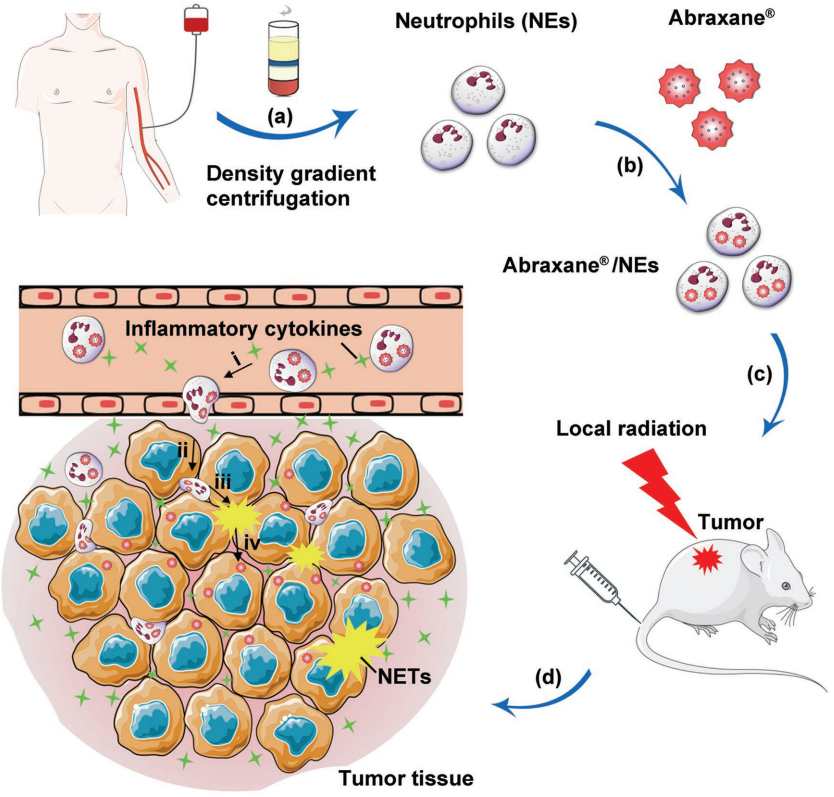


**Figure 1.** Schematic illustration of Abraxane/human NEs cytopharmaceuticals combined with radiotherapy for the suppression of gastric cancer. a) Human NEs are isolated from the peripheral blood of healthy donors using density gradient centrifugation. b) The cytopharmaceuticals Abraxane/NEs are obtained by incubating the isolated NEs with Abraxane. c) Gastric tumor SNU719-bearing nude mice are intravenously administrated of Abraxane/NEs after treatment with modest radiotherapy which amplifies inflammatory signals in tumor sites, thus resulting in enhanced in vivo tumor targeting and superior chemotherapy effect. d) Schematic that shows how Abraxane/NEs target gastric tumor after intravenous injection into mice which have been treated with radiotherapy: (i) Abraxane/NEs are guided by inflammatory cytokines gradient and transmigrate across the vessel wall; (ii) Abraxane/NEs penetrate the tumor tissue along the inflammatory cytokines gradient; (iii) Substantial Abraxane/NEs are excessively activated by the concentrated cytokines followed by the NETs formation, which result in a concomitant release of Abraxane; (iv) Abraxane are engulfed by adjacent tumor cells, thus producing an antitumor effect. NETs, the neutrophil extracellular traps, primarily consist of DNA from NEs which are excessively activated by inflammatory cytokines.

## 2. Results and Discussion

### 2.1. Isolation and Characterization of Human Mature NEs

Human NEs, the most abundant white blood cells in peripheral blood, possess the natural chemotaxis to inflammatory signals and act as the frontline defender against pathogens.[10] In this paper, mature human NEs were isolated from the peripheral blood of healthy donors and purified by density-gradient centrifugation with a yield of about $2 \times 10^6$ cells $mL^{-1}$ blood according to the modified method previously described.[15] The purity was quantified to exceed 90% based on the expression level assay of the mature human NEs-specific biomarkers including CD66b and CD16 (Figure S1A, Supporting Information).[16] The confocal laser scanning microscopy (CLSM) images showed the typical segmented nucleus structure of the living neutrophils (Figure S1B, Supporting Information). Morerover, the expression level of CD11b, an NE-specific surface protein, dramatically increased after incubation with $50 \times 10^{-9}$ M phorbol-12-myristate-13-acetate (PMA) as the simulation of inflammatory factors (Figure S1C, Supporting Information),[17] implying that the purified human NEs were living cells and could be primed rapidly on the occurrence of inflammation.

### 2.2. Radiotherapy Induced Tumor-Targeting of Human NEs

To investigate whether radiotherapy is able to induce the enlargement of inflammatory signals and improve the in vivo tumor-targeting ability of the reinfused


© 2018 WILEY-VCH Verlag GmbH & Co. KGaA, Weinheim

human NEs, we first labeled the purified human NEs with membrane dye DiR (DiR-NEs) for intuitive observation using the in vivo fluorescence imaging system. The in vivo biodistribution of DiR-NEs was monitored after intravenous injection into SNU719 tumor-bearing mice whose tumor had been exposed to different radiation doses of 2, 5, and 10 Gy 24 h before injection, and further confirmed by a quantitative region of interest (ROI) analysis (**Figure 2**A; Figure S2, Supporting Information). With the increase of radiation dose, DiR-NEs exhibited correspondingly enhanced fluorescence signals at tumor sites, confirming that the local radiotherapy could improve the tumor-targeting efficiency of the infused human NEs according to the radiation dose. Thereinto, treatment with 2 Gy radiation dose showed a delayed and fairly weak tumor accumulation of NEs, while treatment with 5 or 10 Gy radiation dose exhibited a clear fluorescence signal at tumor site at 1 h postinjection and lasted for 48 h (Figure S3, Supporting Information), which demonstrated that both 5 and 10 Gy radiation doses possessed the capability of mass NEs recruitment. Considering the overall tumor-killing effect

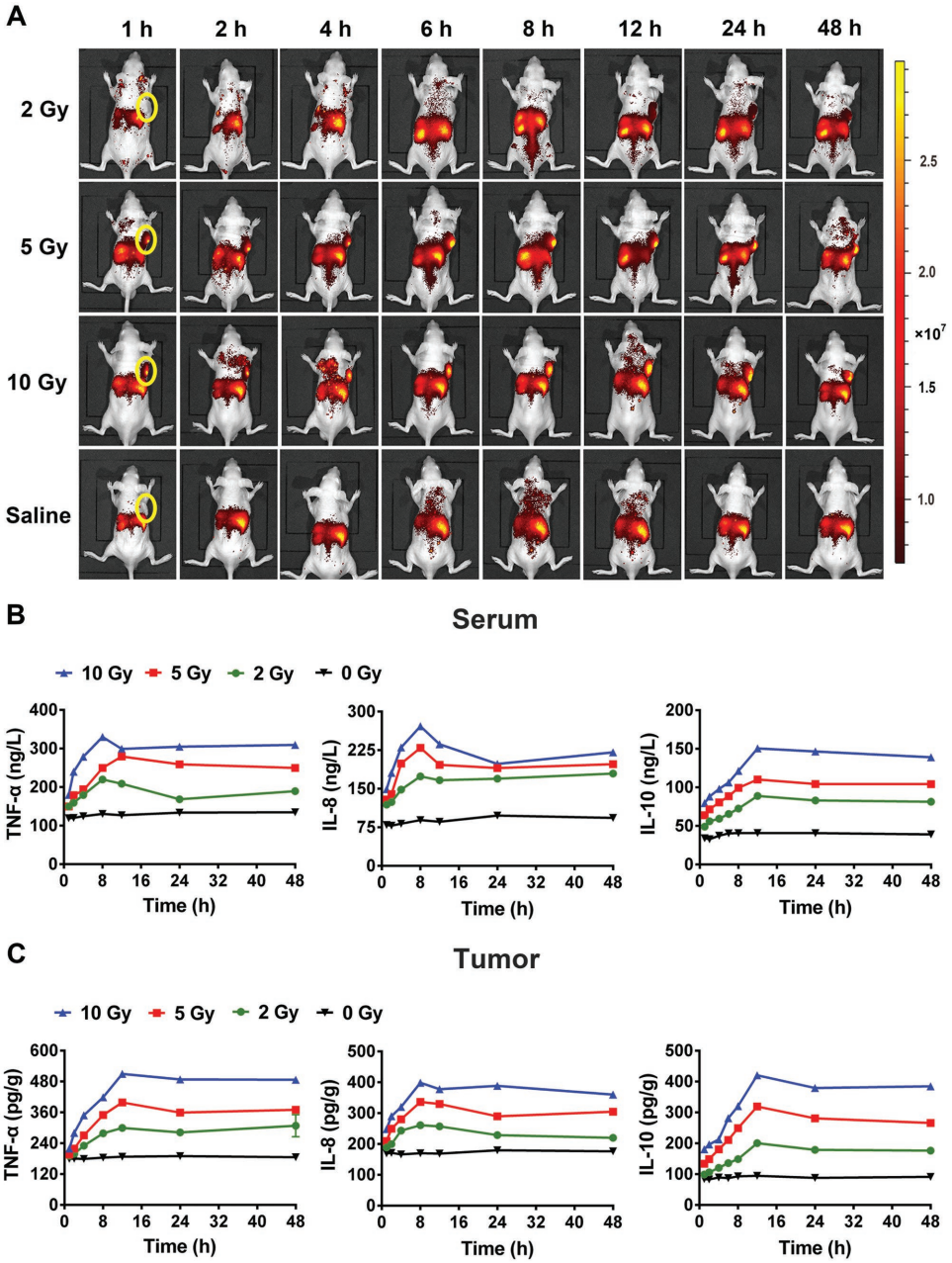


**Figure 2.** Local radiotherapy enhanced NEs migration to the tumor tissues. A) In vivo fluorescence imaging of SNU719 tumor-bearing mice whose tumor has been exposed under different radiation doses after intravenous injection of DiR-labeled purified human NEs at a dosage of $1 \times 10^6$ NEs per mouse. The yellow circles indicate the xenograft tumors. B–C) Expression levels of TNF-$\alpha$, IL-8, and IL-10 in B) serum and C) tumor of SNU719 tumor-bearing mice after local radiotherapy with different radiation doses for 48 h ($n = 3$). All data are shown as mean ± SD.


© 2018 WILEY-VCH Verlag GmbH & Co. KGaA, Weinheim

combined with lower potential side effects, the radiation dose of 5 Gy was more suitable for effective and sustained NEs chemotaxis.

To further explore the specific cause for enhanced NEs chemotaxis from radiotherapy, the expression levels of inflammatory cytokines including IL-8,[18] IL-10,[9a,19] and tumor necrosis factor (TNF-$\alpha$)[20] were quantified in the serum and tumor of SNU719-bearing mice after local radiotherapy (Figure 2B,C). All the expression levels of inflammatory cytokines were upregulated and lasted for 48 h due to the local radiation exposure, manifesting that an inflammatory stress reaction occured after local radiotherapy and the increased amounts of the correlative cytokines were retained in the tumor for a long period. Moreover, the peak concentrations of IL-8, IL-10, and TNF-$\alpha$ induced by 5 Gy dose were 1.32-fold, 1.24-fold, and 1.27-fold in the serum and 1.29-fold, 1.59-fold, and 1.33-fold in the tumor higher than 2 Gy dose, respectively. This result further verified that the amplified inflammatory factors were closely related to the radiotherapy, which was thus more beneficial for NEs recruitment. Taken together, these relevant inflammatory cytokines upregulated by radiation exposure resulted in an elevated tumor-targeting effect of human NEs, which laid the foundation for in vivo application of human NEs as an enhanced tumor-targeting carrier.

### 2.3. Safety Evaluation of Human NEs

Despite the endogenous human NEs are considered to have superior biocompatibility, the potential risk of amounts of human NEs reinfused into the body as vectors is still inconclusive. For evaluating the biological safety of human NEs after intravenous administration, the blood routine and biochemical indexes assay were performed on healthy nude mice at the 3rd day and 30th day, respectively, which had received five-day successive injections of different doses of human NEs before. As shown in **Figure 3**A and Figure S4A (Supporting Information), there was a significant reduction in counts of blood cells including leukocytes, lymphocytes, platelets, neutrophils, and monocytes when mice received a high dose of $6 \times 10^6$ NEs at the 3rd day, which probably resulted from the blood toxicity induced by excess exogenous immunological cells. And unfortunately, all the mice in the high dose of $6 \times 10^6$ NEs were sacrificed at the 30th day. By contrast, no substantial decrease in counts of blood cells was observed in mice after treatment with $3 \times 10^6$ NEs and $1.5 \times 10^6$ NEs for a longer term (Figure 3B; Figure S4B, Supporting Information), which indicated a dose-dependent blood toxicity of human NEs. It was worth noting that the counts of platelets temporarily declined at the 3rd day and recovered to the normal level at the 30th day, confirming the better biological safety of human NEs under the toxic threshold. Moreover, the blood expression levels of aspartate aminotransferase (AST), alanine aminotransferase (ALT), alkaline phosphatase (ALP), the creatinine (Cre), and blood urea nitrogen (BUN) of mice were stable (Figure 3C,D; Figure S5, Supporting Information), reflecting that the infused human NEs did no harm to the normal organs, which was further verified by the histological images of the haematoxylin and eosin (H&E)-stained normal tissues sections (Figure S6, Supporting Information). In general, these data indicated that human NEs could serve as a relatively safe carrier for in vivo application when the dosage was no more than $3 \times 10^6$ NEs per mouse.

### 2.4. Preparation and Characterization Abraxane/NEs

Although it has been confirmed that human NEs with better biological safety can actively target the tumor site in response to local radiation, the drug-loading capability of human NEs is uncertain. To verify the potential capability of human NEs to be a highly effective vector, the commercial nanodrug Abraxane was incubated with the purified human NEs to form cytopharmaceuticals named as Abraxane/NEs. Before loading with Abraxane, the toxicity of Abraxane to human NEs was studied by methyl thiazolyl tetrazolium (MTT) assay (Figure S7, Supporting Information). Within 12 h of incubation, Abraxane of different concentrations had negligible toxicity toward NEs owing to the decreased release of PTX from Abraxane and the absent proliferation ability of mature NEs,[21] as the anticancer mechanism of PTX in Abraxane is to inhibit cell proliferation. Afterward, we optimized the incubation concentration and time of Abraxane with human NEs (Figure S8, Supporting Information), resulting in a high loading capacity of Abraxane/NEs with 18 μg PTX per $1 \times 10^6$ NEs. The encapsulated Abraxane was uniformly dispersed within the human NEs observed by CLSM (Figure S9, Supporting Information). The in vitro stability of Abraxane/NEs was explored under different conditions including PBS (pH 7.4) to mimic a storage medium in vitro (**Figure 4**A) and human plasma to imitate a physiological environment in vivo (Figure 4B). As time extending, the PTX amount in NEs declined slowly while rose gradually in phosphate buffer solution (PBS). However, the PTX amount in NEs was basically stable for 4 h, suggesting that the cytopharmaceuticals should be administrated as soon as possible after preparation. The sharply decreased PTX in NEs at 6 h was probably ascribed to the degradation by abundant enzymes in human NEs. Similarly, Abraxane/NEs showed a consistent tendency of change in PTX amount after incubation with human plasma for 6 h compared with PBS, which implied that the cytopharmaceuticals could stable in vivo within 6 h. Even if the Abraxane released at 6 h, it might have arrived at the tumor sites and acted on the tumor cells according to the in vivo fluorescence images that amounts of NEs had accumulated at tumor sites since 1 h after injection.

### 2.5. Assessment of the Physiological Functions of Abraxane/NEs

Given that the physiological functions of NEs were essential for in vivo migration, the physiological functions of Abraxane/NEs such as phagocytosis as body-defenders and other functions in response to inflammatory factors were evaluated, including chemotaxis, superoxide generation, transendothelial migration, and the NETs formation. The flow cytometry indicated that there was no difference in the capacity of necrotic cells engulfment between Abraxane/NEs and free NEs (Figure S10, Supporting Information). Next, a transwell migration assay confirmed that Abraxane/NEs could be activated by


© 2018 WILEY-VCH Verlag GmbH & Co. KGaA, Weinheim

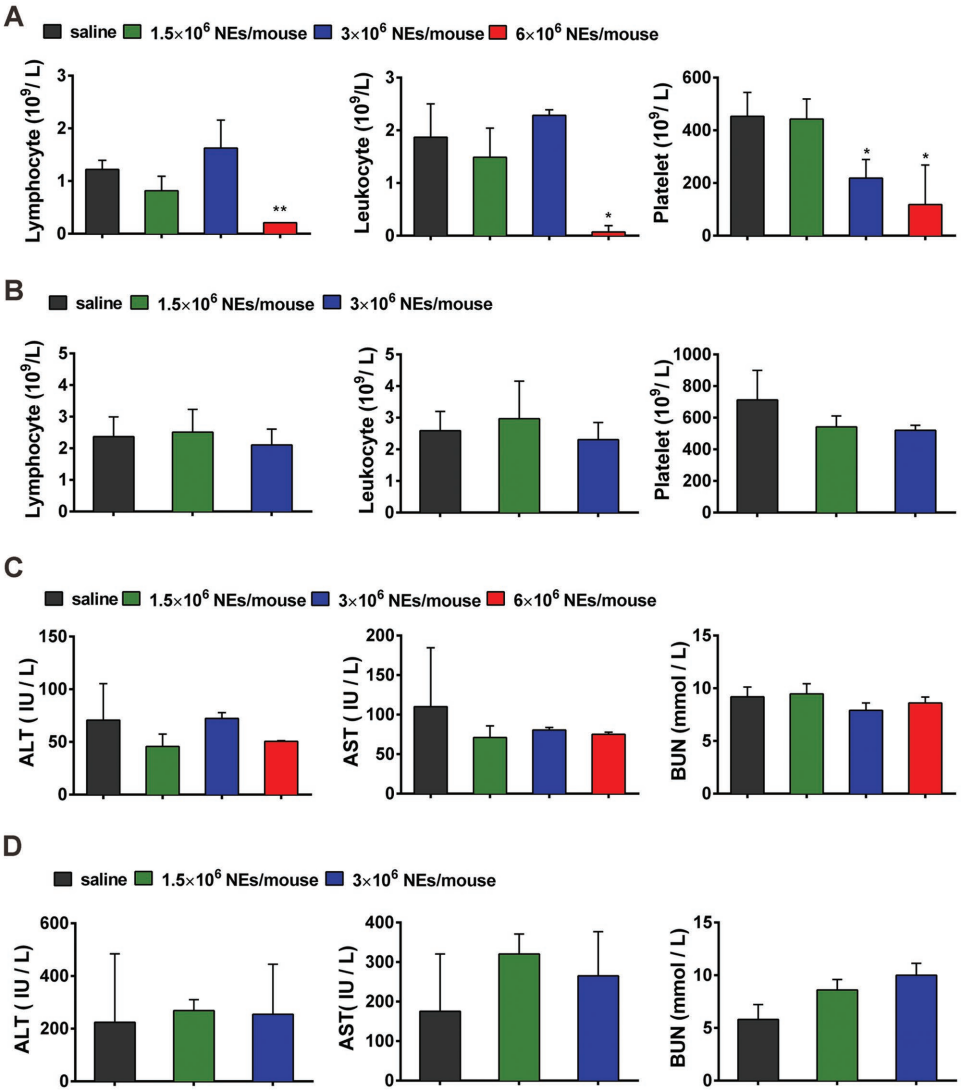


**Figure 3.** Safety evaluation of human NEs intravenously injected into the nude mice at different dosages ($n = 6$). A,B) Haemocytes counts including leukocytes, lymphocytes, and platelets of nude mice at A) the 3rd day and B) 30th day, which have received five-day successive injections of different doses of human NEs. $^*P < 0.05$, $^{**}P < 0.01$. C,D) Blood biochemical indexes including AST, ALT, and BUN of nude mice at C) the 3rd day and D) 30th day, which have received five-day successive injections of different doses of human NEs. AST: aspartate aminotransferase. ALT: alanine aminotransferase. BUN: blood urea nitrogen.

formylmethionyl leucyl phenylalanine (fMLP), an NEs chemotactic peptide,[17] presenting a fMLP concentration-dependent chemotaxis comparable to that of human NEs (Figure 4C; Figure S11, Supporting Information). Furthermore, Abraxane/NEs treated with fMLP exhibited a significantly increased level of superoxide anion, which showed a similar effect with human NEs (Figure S12, Supporting Information).

To evaluate the transendothelial capability of Abraxane/NEs, a human umbilical vein endothelial cells (HUVEC) monolayer was well-established as an in vitro vascular wall model with the transepithelial electrical resistance (TEER) values over 300 $\Omega$ cm$^{-2}$ (Figure 4D). Under the inflammatory conditions simulated by fMLP, about 42% Abraxane/NEs were found in the lower chamber without substantial difference with human NEs (Figure 4E). To be specific, the quantity of PTX delivered by Abraxane/NEs across the monolayer was about 39% (Figure 4F), manifesting that the prepared cytopharmaceuticals could successfully carry the encapsulated nanodrug across the blood vessel in response to fMLP,[22] whereas less than 1% PTX was detected in the lower chamber without the fMLP-activated chemotaxis (Figure 4G). As expected, Abraxane without the aid of NEs demonstrated extremely low permeability through the monolayer regardless of the presence of fMLP due to the tight junctions between neighbouring endothelial cells.

At the end, we evaluated the NETs formation of Abraxane/NEs after treatment with $100 \times 10^{-9}$ M PMA for 4 h using CLSM. The CLSM image of Abraxane/NEs displayed the NETs formation with the blue filiform fluorescence of extracellular DNA stained with hoechst, similar to that of unloaded NEs (Figure 4H). Collectively, Abraxane/NEs maintain the physiological functions of human NEs, which can respond to the inflammatory stimulation, actively migrate across the blood


© 2018 WILEY-VCH Verlag GmbH & Co. KGaA, Weinheim

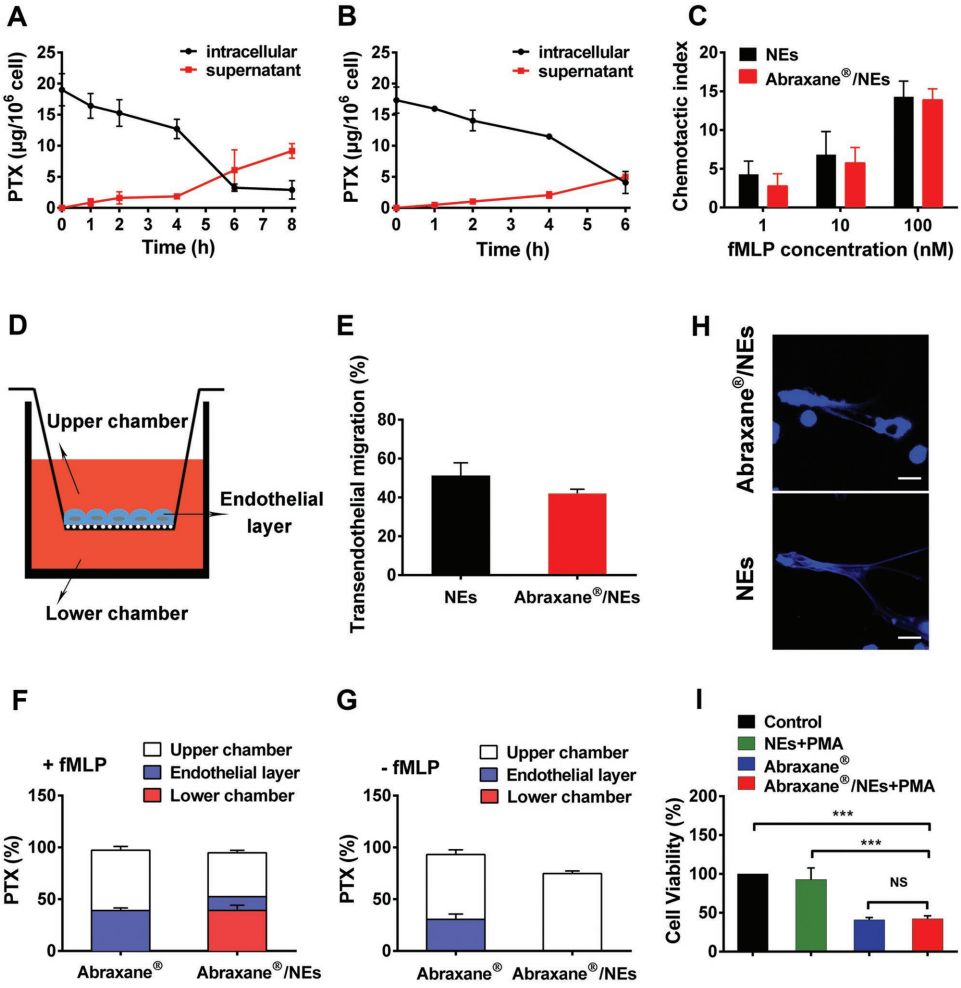


**Figure 4.** Characterization and evaluation of Abraxane/NEs. A,B) Determination of the amount of PTX released from and retained in Abraxane/NEs after incubation A) with PBS or B) with human plasma over time, respectively ($n = 3$). C) The chemotaxis activity of NEs and Abraxane/NEs under different fMLP concentrations ($n = 3$). D) Schematic illustration of the in vitro blood wall model using a transwell chamber for the transendothelial assay of Abraxane/NEs. E) The transendothelial ratios of NEs and Abraxane/NEs in the presence of $10 \times 10^{-9}$ M fMLP ($n = 3$). F,G) Quantification of the PTX distribution in the transwell chamber after incubation with Abraxane and Abraxane/NEs F) in the presence of fMLP and G) in the absence of fMLP ($10 \times 10^{-9}$ M) for 3 h ($n = 3$). H) The CLSM images of NETs released from Abraxane/NEs (upper) and NEs (lower) after incubation with $100 \times 10^{-9}$ M PMA for 4 h. The extracellular DNA was stained with blue Hoechst 33 258. Bar: 10 μm. I) The in vitro antitumor effect of the Abraxane releasing from Abraxane/NEs after incubation with $100 \times 10^{-9}$ M PMA for 4 h ($n = 6$). ***$P < 0.001$. All data are shown as mean ± SD.

vessel to the inflammation sites and be excessively activated to produce the NETs along with the payload release.

### 2.6. In Vitro Cytotoxicity of Abraxane/NEs

To verify the anticancer effect of Abraxane releasing from Abraxane/NEs, an MTT assay was performed on the human gastric carcinoma SNU-719 cells after a 72 h incubation with the supernatant medium of Abraxane/NEs activated by $100 \times 10^{-9}$ M PMA (Figure 4I). The untreated cells and the cells incubated with the supernatant medium of activated NEs were applied as controls. Compared with the control groups, Abraxane releasing from Abraxane/NEs exhibited a robust cytotoxicity against tumor cells, which was comparable with the fresh Abraxane (equivalent 8 μg mL$^{-1}$ PTX). These data suggested that the packaged Abraxane could be released from Abraxane/NEs probably due to the NETs formation and had the superior toxicity against tumor cells, reflecting the potential of human NEs to be ideal vectors for nanodrugs. Accordingly, the fabricated cytopharmaceuticals have the capacity to accumulate at tumor sites on account of the local radiotherapy-induced inflammatory stimulation and release the Abraxane payload accompanied by the NETs formation for efficient tumor chemotherapy.

### 2.7. In Vivo Therapeutic Effect and Safety Evaluation of Abraxane/NEs Combined with Local Radiotherapy

The therapeutic potential of Abraxane/NEs was evaluated on the SNU-719 tumor-bearing mice after treatment with 5 Gy radiotherapy combined with intravenous administration of Abraxane/NEs at a dosage of equivalent 2.7 mg kg$^{-1}$ PTX according to the administration regimen (**Figure 5**A). Compared with saline as a


© 2018 WILEY-VCH Verlag GmbH & Co. KGaA, Weinheim

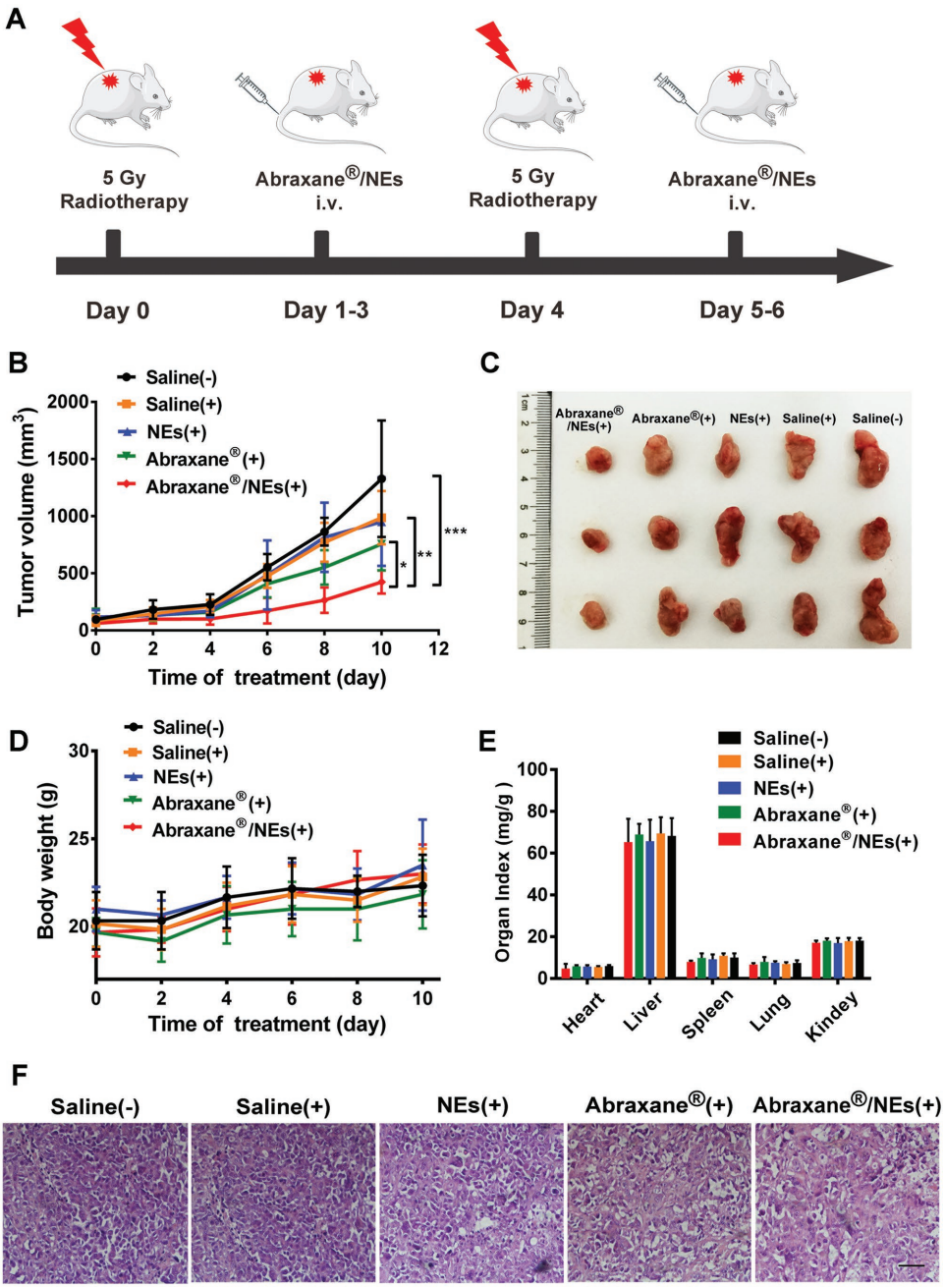


**Figure 5.** Evaluation of the in vivo antitumor effect mediated by the local radiotherapy and Abraxane/NEs. A) Schematic illustration of the administration regimen. B) The SNU-719 tumor growth curves after treatment of the local radiotherapy and the following intravenous injection of different formulations ($n = 6$). *$P < 0.05$, **$P < 0.01$, ***$P < 0.001$. C) Representative images of the isolated SNU-719 xenograft tumors of the mice after treatment at day 12. D) The change in body weights of SNU-719 tumor-bearing mice after treatment over time ($n = 6$). E) The main organ indexes of SNU-719 tumor-bearing mice after treatment at day 12 ($n = 6$). F) Histological observation of the isolated SNU-719 xenograft tumors after treatment. The tumor sections are stained with H&E. Scale bar: 100 µm. (+): with 5 Gy radiotherapy; (–): without 5 Gy radiotherapy. All data are shown as mean ± SD.

negative control, the tumor growth was remarkably suppressed after treatment of local radiotherapy and the following injection of various formulations including saline, NEs, Abraxane, and Abraxane/NEs (Figure 5B,C; Figures S13 and S14, Supporting Information). Under the same radiotherapy conditions, NEs generated a similar inhibitory effect on tumor growth with saline, implying that the infused human NEs lacked the antitumor capability. In comparison, Abraxane group exhibited a noticeable high effect on tumor suppression mainly owing to the chemotherapy effect of nanoscale Abraxane and the local radiotherapy. It was worth noting that Abraxane/NEs group demonstrated a more significant effect on tumor inhibition than Abraxane, which primarily resulted from the highly improved tumor targeting efficiency of Abraxane with the aid of the human


© 2018 WILEY-VCH Verlag GmbH & Co. KGaA, Weinheim

NEs activated by the amplified radiotherapy-induced inflammatory factors. Despite the neutrophils have been reported to be involved in the pathophysiological process of tumor progression and metastasis,[23] the combined antitumor effect of cytopharmaceuticals loaded with Abraxane and local radiotherapy can surmount the possible undesired effect of little amount of the infused neutrophils compared to the whole neutrophils.

The body weights (Figure 5D) and the main organ indexes (Figure 5E) of mice receiving local radiotherapy and Abraxane/NEs remained stable, showing no substantial differences with that of other groups. The histologic images of the tumor sections stained by H&E exhibited a massive cancer cell remission after applying local radiotherapy and Abraxane/NEs (Figure 5F), which further confirmed the efficacy of the combined therapy of local radiotherapy and Abraxane/NEs. Also, no pathological changes were observed from the H&E staining images of the main organs sections (Figure S15, Supporting Information). Taken together, it has verified that Abraxane/NEs can efficiently deliver and release the commercial nanodrug at tumor sites in response to the local radiotherapy which offers an enlarged inflammatory signal, and thereby accomplishes the optimal combined anticancer efficacy.

## 3. Conclusion

In summary, we have developed a neoadjuvant therapy based on Abraxane/human neutrophils cytopharmaceuticals with radiotherapy for effective gastric cancer treatment. Unlike traditional combination therapy that radiotherapy and chemotherapy perform its antitumor activity independently, the cytopharmaceuticals possess the capacity to recognize the amplified radiotherapy-induced inflammatory signals, actively accumulate at the tumor site, and deliver the commercial nanodrug to the cancer cells, thus resulting in a radiotherapy-induced targeting chemotherapy. The combined chemo-radiotherapy has demonstrated superior inhibitory effect on tumor growth, which indicates that the amplification of inflammatory signals after local radiotherapy facilitates the enhancement to the tumor targeting and therapeutic efficacy of Abraxane/NEs. More importantly, human NEs have been confirmed as safe and potential carriers for commercial nanodrugs, which may broaden the clinical applications of nanodrugs on the market. Moreover, the human neutrophils can be extracted from the healthy donors with matched-type or the patients themselves after the injection of granulocyte colony-stimulating factor, futher demonstrating the potential application of human neutrophils. We believe that this neoadjuvant therapy based on cytopharmaceuticals will offer new opportunities for antineoplastic protocols, which may have huge potentials in clinical application in the future.

## 4. Experimental Section

*Materials*: Percoll was purchased from SunShine Biotechnology Co., Ltd. (Nanjing, China). Abraxane (nanoparticle albumin-bound paclitaxel) was purchased from Celgene Corporation (USA). Rhodamine 123 and nuclear fluorescent dye propidium iodide (PI) were purchased from Beyotime Biotechnology (Shanghai, China). N-formyl-L-methionyl-L-leucyl-L-phenylalanine tripeptide (fMLP) and PMA were purchased from Sigma-Aldrich (Shanghai, China). Dihydroethidium (DHE) was purchased from Beyotime Biotechnology (Shanghai, China). Cell-membrane dye DIR was purchased from Life Technologies (Invitrogen). Cell-nucleus dye Hoechst was purchased from Beyotime (China). Enzyme linked immunosolid assay (ELISA) kit was purchased from Elabscience Biotechnology Co.,Ltd (Elabscience). Phycoerythrin (PE)-conjugated human CD16 antibody, fluorescein isothiocyanate (FITC)-conjugated human CD66b antibody, and FITC-conjugated CD11b antibody were all obtained from BioLegend. Fetal bovine serum (FBS), Dulbecco's modified Eagle medium (DMEM) high-glucose medium, trypsin, and penicillin–streptomycin were all obtained from Thermo Fisher Scientific Inc. (Hyclone).

*Cell Lines*: HUVEC cells were purchased from the American Type Culture Collection. SNU719 cells were provided by Drum Tower Hospital (Nanjing, China). All the cells were used without further authentication, but were routinely tested for mycoplasma contamination. HUVEC cells were cultured in DMEM high-glucose medium and SNU719 cells were cultured in Roswell Park Memorial Institute (RPMI) modified medium at 37 °C in a humidified environment containing 5% $CO_2$. All the mediums were supplemented with 10% FBS (v:v), penicillin (100 U $mL^{-1}$), and streptomycin (100 µg $mL^{-1}$).

*Isolation and Characterization of Human Mature NEs*: The human peripheral blood samples were obtained from health donors by centrifugation at 300 g for 20 min at room temperature aseptically. All the experiments were performed in compliance with the Guide for Use of Human Blood, approved by the Ethics Committee of China Pharmaceutical University. All the donors had been informed before the experiments. 6% Dextran T-500 was added to the remaining component with gentle mixing after supernatant discarded. The mixture was placed stably for 30 min at room temperature, followed by removing the supernatant. Then the bottom layer was centrifuged at 300 g for 3 min and resuspended in PBS. The unicellular suspension was added into a Percoll mixture solution consisting of 55, 65, and 78% (v:v) Percoll in PBS, followed by centrifugation at 500 g for 30 min. The mature NEs were recovered at the interface of the 65 and 78% fractions and washed by ice-cold PBS thrice. The viability of the obtained mature NEs was calculated by trypan blue exclusion, and the purity was determined using immunofluorescence double staining with FITC-conjugated human anti-CD16 antibody and PE-conjugated human anti-CD66b antibody by flow cytometry (Accuri C6 flow cytometer, BD Biosciences). The nuclear morphologies of NEs stained with Hoechst 33 258 were observed by laser scanning confocal microscopy (ZEISS). The inflammation-responsive expression of CD11b on NEs was determined using immunofluorescence staining with FITC-conjugated human anti-CD11b antibody after human NEs were incubated with PMA ranging from 0 to $100 \times 10^{-9}$ M for 30 min.

*Animals and Ectopic Gastric Cancer Model*: The nude mice (BALB/c, male, six-weeks old) were provided by the Comparative Medicine Center of Yangzhou University. All the animals were treated in accordance with the Guide for Care and Use of Laboratory Animals, approved by the Animal Experimentation Ethics Committee of China Pharmaceutical University.

Ectopic gastric cancer models were set up by inoculating SNU-719 cells at a concentration of $10^7$ cells $mL^{-1}$ into the armpit of the right forelimb of male BALB/c nude mice for three weeks until the tumor volume up to 100 $cm^3$. Tumor volume ($V$) was determined by measuring length ($L$) and width ($W$) by a vernier caliper and calculated according to the following formula: $V = L \times W2/2$.

*Radiotherapy Induced Tumor-Targeting of Human NEs*: To observe the NEs biodistribution in tumor-bearing mice under radiotherapy, four groups of tumor-bearing nude mice ($n = 3$) separately received different dosages radiotherapy including 0, 2, 5, and 10 Gy. After 24 h, DiR-labeled NEs were intravenously injected into mice and observed at 1, 2, 4, 6, 8, 12, 24, and 48 h postinjection using the in vivo fluorescence imaging system. The fluorescence intensity in the ROI of tumor sites for each mouse was quantitatively measured by in vivo fluorescence imaging system (PerkinElmer, USA). The retention duration of accumulated NEs in tumor was observed separately at 1 h, 2 h, 4 h, 6 h, 8 h, 12 h, 24 h, 48 h, 3 d, 6 d, and 8 d postinjection after 5 Gy radiotherapy for 24 h under the in vivo fluorescence imaging system.

*Detection of Inflammatory Cytokines Expression under Different Radiotherapy Dosages*: The inflammatory cytokines IL-8, IL-10, and TNF-$\alpha$ in the tumor sites and blood of tumor-bearing mice whose tumor


© 2018 WILEY-VCH Verlag GmbH & Co. KGaA, Weinheim

had been exposure on different radiotherapy dosages for 5 min were determined using ELISA method. The blood samples were naturally coagulated, then centrifuged at 13 000 g for 20 min to obtain serum. The tumor tissues were harvested and weighed, then the supernatant was obtained from tissue homogenate in saline by a centrifugation at 13 000 g for 20 min. The quantitative analysis of inflammatory cytokines was manipulated using corresponding ELISA kits (Elabscience).

*Safety Evaluation of Human NEs*: The healthy nude mice were divided into four groups, and intravenously injected with saline and three dosages of NEs once a day for 5 days. Then mice at the 3rd day and 30th day postinjection were separately sacrificed and blood samples harvested were detected by whole blood analyzer. The main blood biochemical parameters for evaluating the functions of mice liver and kidney were as follows: ALT, AST, ALP, BUN, and creatinine (Cre). Histological analysis of normal organs, including the heart, liver, spleen, lung, kidney, and stomach with H&E staining were observed by an optical microscope (Ts2R, Nikon).

*Cytotoxicity of Abraxane toward NEs*: The NEs in the FBS-free 1640 medium were cultured in 24-well plate ($1 \times 10^5$ cells per well) for 1 h, which then were incubated with 200 µL Abraxane of different concentrations in each well for 12 h, followed by adding 20 µL MTT (0.5 mg $mL^{-1}$, Beyotime) in each well. After 4 h of incubation, the medium was removed and 150 µL dimethyl sulfoxide (DMSO) was added into each well. The absorbance was measured at 570 nm by a microplate reader (Multiskan MK3, Thermo Scientific).

*Preparation and Characterization of Abraxane/NEs*: Abraxane/NEs were obtained by incubating Abraxane with NEs. Briefly, the mature NEs ($1 \times 10^5$ cells $mL^{-1}$) were put in a sterile tube, and incubated with different concentrations of Abraxane (Celgene) dilution for predetermined time at 37 °C in a humidified environment containing 5% $CO_2$. After washing with ice-cold PBS thrice, Abraxane/NEs suspension were obtained and used immediately for the subsequent study. To quantify the amount of PTX in the Abraxane/NEs, Abraxane/NEs were disrupted by a cell lysis buffer (Beyotime) to release PTX from the NEs. The cell lysate was collected and centrifuged at 10 000 g for 5 min. The supernatant (50 µL) was mixed with 200 µL of acetonitrile, vortexed for 5 min and centrifuged at 10 000 g for 10 min.

The in vitro stability of Abraxane/NEs was evaluated under different conditions, including the normal physiological condition (PBS, pH 7.4) and human plasma. Briefly, Abraxane/NEs ($1 \times 10^6$ cells per well) were seeded in 24-well plates, and then incubated with PBS or human plasma for different periods (0, 2, 4, 6, and 8 h). The amounts of PTX in the NEs and released in the supernatant medium were determined using high performance liquid chromatography (HPLC).

*Evaluation of Physiological Functions of Abraxane/NEs*: To investigate the phagocytic function of Abraxane/NEs, freshly isolated human NEs ($1 \times 10^5$ cells $mL^{-1}$) were incubated in 56 °C water for 30 min to prepare necrotic cells, which were then incubated with red fluorescent probe PI (2.5 mg $mL^{-1}$, Beyotime) for 30 min. After washing with precold PBS thrice, the dyed necrotic cells were resuspended in FBS-free 1640 medium. Abraxane/NEs were dyed with green fluorescent probe Rhodamine 123 (Beyotime) for 30 min, which were resuspended in FBS-free 1640 medium ($1 \times 10^5$ cells $mL^{-1}$), and then coincubated with dyed necrotic cells in a ratio of 1:1 (vol:vol) for 30 min. Meanwhile, blank NEs were dyed with Rhodamine 123 as a blank control. After washing with precold PBS thrice, the cell pellets were collected and analyzed by flow cytometry (Accuri C6 flow cytometer, BD Biosciences).

The chemotactic function was investigated by a transwell migration assay. The transwell polycarbonate membrane is 3 µm in pore size, 6.5 mm in diameter, and 0.33 $cm^2$ in membrane surface area (Corning). Abraxane/NEs ($1 \times 10^6$ cells $mL^{-1}$) were added into each upper transwell chamber. Different concentrations of the chemotaxin fMLP (Sigma) were respectively added to the lower chamber. Meanwhile, blank NEs in the upper chamber and fMLP-free medium in the lower chamber were respectively set as controls. After incubation for 30 min, the number of NEs through chemotatic migration to the lower chamber was counted using the hemacytometer (Bright-Line, Sigma). The chemotaxis index $[(N_{fMLP} - N_{blank})/N_{blank}]$ was calculated, where $N_{fMLP}$ and $N_{blank}$ are the number of NEs in the lower chamber with fMLP or not.

The inflammation-mediated superoxide generating capability of Abraxane/NEs was evaluated using superoxide indicator DHE (Beyotime). Abraxane/NEs and blank NEs were separately incubated with $1 \times 10^{-6}$ M fMLP for 30 min (5% $CO_2$, 37 °C), followed by washing with PBS thrice. Then the cells were resuspended in FBS-free 1640 medium and incubated with DHE for 30 min (5% $CO_2$, 37 °C). The fluorescent intensity was measured using flow cytometry (Accuri C6 flow cytometer, BD Biosciences). Abraxane/NEs and blank NEs in the medium without fMLP were also set as controls.

To evaluate the capability of chemotactic migration across the blood vessel, we first constructed the in vitro blood vessel model with HUVEC cells using a transwell cell culture system. Briefly, HUVEC cells ($1 \times 10^5$ cells) were seeded into the upper transwell chamber, and the culture medium containing 10% FBS (v:v) was added into the lower chamber. When the value of the TEER detected by a Millicell-ERS voltohmmeter (Millipore) of HUVEC monolayers exceeded 300 Ω $cm^2$, it indicated that the blood vessel models were successfully constructed. Then, Abraxane/NEs ($1 \times 10^6$ cells $mL^{-1}$) and blank NEs ($1 \times 10^6$ cells $mL^{-1}$) were added into each upper transwell chamber, respectively, and 800 µL medium with $10 \times 10^{-9}$ M fMLP was added into the lower chamber. After 3 h of incubation, the number of NEs in the lower chamber was counted as mentioned above.

To further investigate whether drug leakage existed in the migration process, Abraxane/NEs ($1 \times 10^6$ cells $mL^{-1}$) were added into upper transwell chamber and 800 µL medium with $10 \times 10^{-9}$ M fMLP was added into the lower chamber. After 3 h of incubation, Abraxane/NEs in the upper chamber or the lower chamber were collected with centrifugation at 300 g for 3 min, and the middle HUVEC cells monolayer on the transwell membrane were digested with trypsin (200 µL) and centrifuged at 300 g for 3 min. The amount of PTX in collected cells were analyzed with HPLC as mentioned above. In addition, fresh Abraxane (equivalent 18 µg $mL^{-1}$ of PTX) was used as control, in which the subsequent procedure was similar to that for Abraxane/NEs.

To observe the NET formation of NEs and Abraxane/NEs, NEs and Abraxane/NEs ($1 \times 10^6$ cells per well) grown on the glass-bottomed dishes (Corning) were incubated with $100 \times 10^{-9}$ M PMA for 4 h, followed by fixing with 4% paraformaldehyde for 15 min at 4 °C. After washing with PBS thrice, the prepared NETs were stained with the dye Hoechst 33 258 and observed using CLSM (ZEISS).

*In Vitro Cytotoxicity of Abraxane/NEs*: After incubation with PMA ($100 \times 10^{-9}$ M) for 4 h, the supernatant of Abraxane/NEs was collected and analyzed to quantify the amount of PTX in the releasing Abraxane using HPLC. The same amount of commercial Abraxane (equivalent 8 µg $mL^{-1}$ PTX) and the supernatant of fresh NEs incubated with $100 \times 10^{-9}$ M PMA for 4 h were set as control groups.

SNU-719 cells ($1 \times 10^4$ cells per well) were seeded on 96 well plate and incubated for 24 h. The medium was replaced by fresh medium and tumor cells were treated with different formulations for 72 h. Cell viability was estimated by MTT assay according to the manufacturer's protocol. In brief, 20 µL of MTT solution (5 mg $mL^{-1}$) was added to each well. After 4 h, the supernatant was removed carefully and 150 µL of DMSO was added. Absorbance of the solution was measured at 570 nm on a microplate reader.

*In Vivo Therapeutic Effect and Safety Evaluation of Abraxane/NEs Combined with Local Radiotherapy*: The tumor-bearing nude mice were randomly divided into five groups ($n = 6$), of which four groups were exposed to radiotherapy (5 Gy) for 5 min. After 24 h, these mice were administrated once a day with saline, blank NEs ($3 \times 10^6$ cells per mice), Abraxane (equivalent 2.7 mg $kg^{-1}$ PTX), and Abraxane/NEs (equivalent 2.7 mg $kg^{-1}$ PTX) for successive three days, respectively. Then, another radiotherapy (5 Gy) was performed on these four groups. After 24 h, the mice in four groups were administrated once a day for another two days. The last group without radiotherapy treatment was only infused with saline for the same duration as a control. Body weights and tumor volumes were measured and recorded every two days. The tumor-bearing mice were sacrificed at 10th day, whose tumor tissues and normal organs were harvested and weighed. For pathology research, paraffin sections of


© 2018 WILEY-VCH Verlag GmbH & Co. KGaA, Weinheim

tumor were stained with H&E and visualized by inverted fluorescence microscope (Olympus, Japan). The organ index was also obtained from the ratio of organ weight/body weight.

## Supporting Information

Supporting Information is available from the Wiley Online Library or from the author.

## Acknowledgements

C.J. and Y.W. contributed equally to this work. This work was supported by the National Natural Science Foundation of China (Grant Nos. 81773664, 81473153, and 81503003), National Basic Research Program of China (Grant No. 2015CB755504), 111 Project from the Ministry of Education of China and the State Administration of Foreign Expert Affairs of China (Grant Nos. 111-2-07 and B17047), Fundamental Research Funds for the Central Universities of China (Grant No. 2632017ZD06), the Open Project of State Key Laboratory of Natural Medicines (Grant No. SKLNMZZCX201811), and "Double First-Class" University project (Grant No. CPU2018GF10). The authors thank public platform of State Key Laboratory of Natural Medicines for assistance with Confocal Microscopy and Flow Cytometry.

## Conflict of Interest

The authors declare no conflict of interest.

## Keywords

Abraxane, cytopharmaceuticals, gastric cancer, human neutrophils, radiotherapy

Received: October 10, 2018
Revised: November 18, 2018
Published online:

[1] a) P. C. Lott, L. G. Carvajal-Carmona, *Lancet Gastroenterol. Hepatol.* **2018**, *3*, 874; b) E. Van Cutsem, X. Sagaert, B. Topal, K. Haustermans, H. Prenen, *Lancet* **2016**, *388*, 2654.

[2] a) R. Sitarz, M. Skierucha, J. Mielko, G. J. A. Offerhaus, R. Maciejewski, W. P. Polkowski, *Cancer Manage. Res.* **2018**, *10*, 239; b) R. Wadhwa, S. Song, J. S. Lee, Y. Yao, Q. Wei, J. A. Ajani, *Nat. Rev. Clin. Oncol.* **2013**, *10*, 643.

[3] a) T. T. Zhao, H. Xu, H. M. Xu, Z. N. Wang, Y. Y. Xu, Y. X. Song, S. C. Yin, X. Y. Liu, Z. F. Miao, *Gastric Cancer* **2018**, *21*, 361; b) M. A. Molinaro, *Radiother. Oncol.* **2005**, *76*, S46.

[4] T. Yoshikawa, Y. Rino, N. Yukawa, T. Oshima, A. Tsuburaya, M. Masuda, *Surg. Today* **2014**, *44*, 11.

[5] a) M. Valkov, S. Asakhin, M. Levit, O. Vtoraya, A. Ruzhnikova, S. Litinskiy, *Eur. J. Cancer* **2011**, *47*, S454; b) G. A. Davids, R. Glynne-Jones, *Clin. Oncol.* **2000**, *12*, 246; c) W. Deng, W. Chen, S. Clement, A. Guller, Z. Zhao, A. Engel, E. M. Goldys, *Nat. Commun.* **2018**, *9*, 2713; d) Y. Chao, L. G. Xu, C. Liang, L. Z. Feng, J. Xu, Z. L. Dong, L. L. Tian, X. Yi, K. Yang, Z. Liu, *Nat. Biomed. Eng.* **2018**, *2*, 611; e) X. J. Song, J. Xu, C. Liang, Y. Chao, Q. T. Jin, C. Wang, M. W. Chen, Z. Liu, *Nano Lett.* **2018**, *18*, 6360.

[6] a) N. Zhao, Z. Zeng, Y. Zu, *Small* **2018**, *14*, 1702103; b) S. Y. Qin, A. Q. Zhang, X. Z. Zhang, *Small* **2018**,*14*, 1802417.

[7] T. Fujita, *Lancet Oncol.* **2013**, *14*, 440.

[8] a) H. Ma, Y. Liu, M. Shi, X. Shao, W. Zhong, W. Liao, M. M. Xing, *Biomacromolecules* **2015**, *16*, 4022; b) R. Li, B. Liu, J. Gao, *Cancer Lett.* **2017**, *386*, 123; c) Z. Yang, H. Luo, Z. Cao, Y. Chen, J. Gao, Y. Li, Q. Jiang, R. Xu, J. Liu, *Nanoscale* **2016**, *8*, 11543.

[9] a) J. W. Xue, Z. K. Zhao, L. Zhang, L. J. Xue, S. Y. Shen, Y. J. Wen, Z. Y. Wei, L. Wang, L. Y. Kong, H. B. Sun, Q. N. Ping, R. Mo, C. Zhang, *Nat. Nanotechnol.* **2017**, *12*, 692; b) Z. Xie, Y. Su, G. B. Kim, E. Selvi, C. Ma, V. Aragon-Sanabria, J. T. Hsieh, C. Dong, J. Yang, *Small* **2017**, *13*, 1603121; c) L. A. L. Fliervoet, E. Mastrobattista, *Adv. Drug Delivery Rev.* **2016**, *106*, 63; d) J. Si, S. Shao, Y. Shen, K. Wang, *Small* **2016**, *12*, 5108.

[10] a) W. M. Nauseef, N. Borregaard, *Nat. Immunol.* **2014**, *15*, 602; b) N. Borregaard, *Immunity* **2010**, *33*, 657.

[11] a) V. Zorzetto, G. Maddalo, D. Basso, F. Farinati, *Immunotherapy* **2012**, *4*, 587; b) M. Honda, P. Kubes, *Nat. Rev. Gastroenterol. Hepatol.* **2018**, *15*, 206.

[12] a) H. E. Barker, J. T. Paget, A. A. Khan, K. J. Harrington, *Nat. Rev. Cancer* **2015**, *15*, 409; b) D. E. Citrin, Y. J. Hitchcock, E. J. Chung, J. Frandsen, M. E. Urick, W. Shield, D. Gaffney, *Radiat. Oncol.* **2012**, *7*, 64.

[13] a) R. Wesolowski, C. Lee, R. Kim, *Lancet Oncol.* **2009**, *10*, 903; b) K. Shitara, A. Takashima, K. Fujitani, K. Koeda, H. Hara, N. Nakayama, S. Hironaka, K. Nishikawa, Y. Makari, K. Amagai, S. Ueda, K. Yoshida, H. Shimodaira, T. Nishina, M. Tsuda, Y. Kurokawa, T. Tamura, Y. Sasaki, S. Morita, W. Koizumi, *Lancet Gastroenterol. Hepatol.* **2017**, *2*, 277; c) J. Park, J. E. Park, V. E. Hedrick, K. V. Wood, C. Bonham, W. Lee, Y. Yeo, *Small* **2018**, *14*, 1703670.

[14] C. W. Steele, N. B. Jamieson, T. R. Evans, C. J. McKay, O. J. Sansom, J. P. Morton, C. R. Carter, *Br. J. Cancer* **2013**, *108*, 997.

[15] C. Lichtenberger, S. Zakeri, K. Baier, M. Willheim, M. Holub, W. Reinisch, *J. Immunol. Methods* **1999**, *227*, 75.

[16] a) E. Fortunati, K. M. Kazemier, J. C. Grutters, L. Koenderman, J. Van den Bosch v, *Clin. Exp. Immunol.* **2009**, *155*, 559; b) J. A. Andersson, A. Egesten, L. O. Cardell, *Allergy (Oxford, U. K.)*. **2002**, *57*, 718.

[17] V. Brinkmann, U. Reichard, C. Goosmann, B. Fauler, Y. Uhlemann, D. S. Weiss, Y. Weinrauch, A. Zychlinsky, *Science* **2004**, *303*, 1532.

[18] a) E. Kolaczkowska, P. Kubes, *Nat. Rev. Immunol.* **2013**, *13*, 159; b) P. Tabatabaei, E. Visse, P. Bergstrom, T. Brannstrom, P. Siesjo, A. Bergenheim, *J. Neuro-Oncol.* **2017**, *131*, 83.

[19] T. Tokes, G. Varga, D. Garab, Z. Nagy, G. Fekete, E. Tuboly, I. Plangar, I. Man, R. E. Szabo, Z. Szabo, G. Volford, M. Ghyczy, J. Kaszaki, M. Boros, K. Hideghety, *Int. J. Radiat. Biol.* **2014**, *90*, 1.

[20] C. E. Rube, F. Wilfert, D. Uthe, K. W. Schmid, R. Knoop, N. Willich, A. Schuck, C. Rube, *Radiother. Oncol.* **2002**, *64*, 177.

[21] M. Evrard, I. W. H. Kwok, S. Z. Chong, K. W. W. Teng, E. Becht, J. Chen, J. L. Sieow, H. L. Penny, G. C. Ching, S. Devi, J. M. Adrover, J. L. Y. Li, K. H. Liong, L. Tan, Z. Poon, S. Foo, J. W. Chua, I. H. Su, K. Balabanian, F. Bachelerie, S. K. Biswas, A. Larbi, W. Y. K. Hwang, V. Madan, H. P. Koeffler, S. C. Wong, E. W. Newell, A. Hidalgo, F. Ginhoux, L. G. Ng, *Immunity* **2018**, *48*, 364.

[22] D. Feng, J. A. Nagy, K. Pyne, H. F. Dvorak, A. M. Dvorak, *J. Exp. Med.* **1998**, *187*, 903.

[23] a) S. Patel, S. Fu, J. Mastio, G. A. Dominguez, A. Purohit, A. Kossenkov, C. Lin, K. Alicea-Torres, M. Sehgal, Y. Nefedova, J. Zhou, L. R. Languino, C. Clendenin, R. H. Vonderheide, C. Mulligan, B. Nam, N. Hockstein, G. Masters, M. Guarino, Z. T. Schug, D. C. Altieri, D. I. Gabrilovich, *Nat. Immunol.* **2018**, *19*, 1236; b) Z. Castano, B. P. San Juan, A. Spiegel, A. Pant, M. J. DeCristo, T. Laszewski, J. M. Ubellacker, S. R. Janssen, A. Dongre, F. Reinhardt, A. Henderson, A. G. del Rio, A. M. Gifford, Z. T. Herbert, J. N. Hutchinson, R. A. Weinberg, C. L. Chaffer, S. S. McAllister, *Nat. Cell Biol.* **2018**, *20*, 1084.


© 2018 WILEY-VCH Verlag GmbH & Co. KGaA, Weinheim